Encapsulation Surface Roughness Effect on The Performance of Cool Storage Systems

Ahmed A. Altohamy[1.a,b], Ismail M. M. Elsemary[2.a,b], Saber Abdo[3.c] , M.A. Abdelrahman[4.a] , Ahmed A.A. Attia[5.a], R.Y. Sakr[6.a]

[1]Ahmed.soliman@feng.bu.edu.eg, [2]i.semary@feng.bu.edu.eg, [3]Saber.abdo@bristol.ac.uk, [5]Ahmed.attia@feng.bu.edu.eg, [6]Ramadan.sakr@feng.bu.edu.eg

[a] Combustion and Energy Technology Lab, Mechanical Engineering Department, Shoubra Faculty of Engineering, Benha University, Cairo, Egypt

[b] Department of Mechanical Engineering, College of Engineering, Northern Border University, Arar, Saudi Arabia.

[c] Mechanical Engineering Department, University of Bristol, Bristol, UK.

Abstract:

Cool Storage is a well-known technique that been used to increase the energy efficiency of cooling systems. This paper represents a novel experimental work for the effect of internal capsules surface roughness on the performance of encapsulated cool storage systems. In this study, distilled water was used as a phase change material inside capsules. Internal surface roughness of (0, 3, 7 and 12) μm were tested using the same heat transfer fluid Characteristics. Heat transfer fluid (HTF) composed of (50-50) %wt. of (water – Ethylene glycol) was used with a fixed volume flow rate of 12 Litre per Minute LPM and four different inlet temperatures of (-6, -8, -10 and -12)˚C. The solidified mass fraction, charging rate and energy storage were calculated and plotted versus the charging time to determine the surface roughness effect on the cooling performance of the system. Results showed that the internal surface roughness of capsules had adverse effect on the system performance through increasing the total freezing (charging) time. Results also indicated that the charging time increased by (14 to 17) % at inlet flow temperature of (-12 and -6)˚C, respectively at the higher roughness values compared with the smooth surface capsule e.g. Zero roughness parameter.

Key words: Cool storage, PCM, Solidification. Surface roughness

1- Introduction:

Reliable and power-efficient cool thermal storage systems are very important for various applications including food processing, grocery storage, air conditioning systems, pharmaceutical industries, and many other cooling applications. The world energy consumption is increasing on a daily basis due to population increase and technology development. Phase change materials (PCMs) had attracted many researchers to use it in cool storage systems because of its high latent heat. Cool storage systems utilising PCMs showed a promising performance during off-peak times in many test cases. Paraffin wax, RTs, water, and recently Nano fluids are the most used materials in such systems [1] and [2].

PCMs have been studied for many applications due to that latent heat is always more times than sensible heat. These applications included solar energy applications [3], building energy performance improvement [4], and many other heat storage applications.In the last two decades. ice storage systems have been widely studied due to their excellent characteristics of flatting the electric power load curve in the daytime for central air conditioning systems. Most studies in this area focused on heat transfer fluid characteristics such as fluid material, Nano fluid insertion, volume flow rate and fluid temperature. On the other hand, system configuration including capsule geometry, shape and size were also investigated to optimise the system cooling performance [5], [6] and [7].

Said M. A. [8] proposed a novel technique for using PCMs with different configurations with air conditioning systems. Their results stated that the charging time and outlet temperature were

reduced by increasing air speed. They also recommended using thinner and longer configurations of PCMs for shortening the cooling time. Yan C. et al. [9] proposed a study to combine the seasonal cold storage and chilled water storage for usage in small buildings. They also proposed a design optimisation for the compound system. They concluded that using the combination had a significant improvement on the system overall performance. The combination also increased the system applicability and reduced the life cycle cost by 40%.

Many trials have been recently done by researchers to investigate different aspects of system design with different end-uses. Cheng X. and Zhai X. [10] studied experimentally and numerically the thermal performance of a cascaded packed bed cold storage unit. They compared their proposed multiple-stage unit with a single-stage unit of the same type according to different aspects including, thermal performance, charging rate, and exergy efficiency. They recommended using 3-5 stages unit for that type of systems.

From another perspective, Yu Q. et al. [11] investigated the heat transfer behaviour and the mechanical stability of microcapsules while the solidification occurs. They developed a thermo-mechanical model to apply energy conservation equation, Lame's equation, and bucking theory. They studied the effect of shell design parameters including thickness, composition, and size on the pressure difference, freezing point and latent heat of the encapsulated material. They stated that their model was able to predict the experimental behaviour using the applied equations.

Panchabikesan K et al. [12] proposed a modified system to enhance the output of a free cooling system using PCMs. A significant reduction on the charging time of 28.7% and 34.8% was achieved using heat transfer fluid (HTF) of velocities 2 and 1.5 m/s. They stated that their system could be either used as a standalone unit for cooling buildings or as an integration with a conventional HVAC system for improving the overall building cooling performance.

Also other researchers focused on giving more reviews about PCM technologies that could serve the industry especially room air conditioning applications, like Pomianowski et al. [13] who presented a review which stated that water can be used for thermal storage systems. They referred to the water thermal characteristics including high latent heat for evaporation and fusion, chemical stability, availability, and compatibility with air conditioning systems.

In a related study, Safari et al. [14] reviewed the super-cooling problem of PCMs, which is a challenging thermo physical property that makes troubles in thermal storage applications. They also investigated different applications that can use the water super-cooling phenomenon. They developed different techniques for increasing water stability and designed an adequate super-cooled heat storage system. They concluded that the ice storage system can be considered as a powerful, developed and dominant technique for cool storage systems.

Surface roughness is one of the factors that been studied for external ice formation over surfaces. Liu S. et al. [15] investigated the impacts on water solidification over a plate surface using ice slurry. They studied the effect of roughness and inhibitor concentration on both freezing temperature and nucleation energy. Their results indicated that the roughness and concentration significantly affect the freezing temperature of the droplet. By increasing the roughness, the freezing temperature rises, and the nucleation energy drops.

Saito et al. [16] studied the super cooling phenomenon relation with the surface roughness and concluded that the cooling rate and the surface roughness degree were related to the time required for the icing process. Faucheux et al. [17] studied the effect of surface roughness for metal tubes on the super-cooling magnitude during freezing progression. They used three aqueous mixtures of water and

ethanol. The ethanol concentration in the mixture was 5%, 10% and 15% with aluminium tube of five different external surface roughness. They stated that the roughness influences the super cooling process with an adverse effect.

Entering the Nano technology research era encouraged researchers to study nanofluids utilisation in freezing systems. Wang et al. [18] experimentally investigated the usage of Cu-H_2O nanofluid as a cooling storage PCM for cooling systems and their effect on the super-cooling of water PCMs. Experimental results indicated that the Cu-H_2O Nano fluids with different concentration have a lower super-cooling effect compared with water. They also concluded that by increasing the nanoparticles concentration, the freezing time decreased for example: at 0.1 wt.% concentration, the super-cooling degree was 20.5% and total freezing time was 19.2% less than using pure water as a PCM.

Liu et al. [19] studied the nucleation behaviour and the super cooling of Nano fluids when using them as PCMs. They used graphene oxide Nano sheets with deionized water without using surfactants. Their results demonstrated that the super-cooling degree was reduced by 69.1% and the icing time was also reduced by 90.7% compared with deionised pure water. Their study implied that graphene oxide Nano fluids can be promising PCMs in cold storage due to their reduced super-cooling degree and fast nucleation.

Chandrasekaran et al. [20], [21] studied the effect of encapsulation size and the volume filling ratio, respectively on the solidification process of spherical capsules while capsules were filled with deionized water as PCM. They concluded that the degree of sub cooling was decreased with the increase of both capsule filling volume ratio and its size.

From the literature provided above, it can be noted that the research on the cool storage area influenced either studying different parameters affecting the system performance or providing enhancement techniques for cooling systems. These techniques are divided into two main categories. The first one is to improve the thermal characteristics by adding additives (Nano particle, chemical additives, etc...) or creating novel material to enhance the PCM thermal characteristics, hence reducing the freezing time. The second technique is to work on design parameters for example: the capsulation size, shape, capsule material and capsules arrangement. Other design parameters such as heat transfer fluid inlet temperature and volume flow rates were completely and well-studied.

From the literature also it can be concluded that, the internal surface roughness for PCM capsules and its effect on the charging time, power and freezing rate has not been studied yet. This work aims to primary investigate the effect of capsule internal surface roughness using spherical capsule filled **with pure and boiled water as a PCM**. A test rig was manufactured and calibrated to test the effect of different surface roughness on the performance of the cool storage systems.

Nomenclature

C_i	Specific heat of ice, kJ/kg.K
C_w	Specific heat of water, kJ/kg.K
L.H.	Latent heat of fusion of water, kJ/kg.
m_o	Mass of PCM encapsulated inside the spherical capsule, kg
m_s	Solidified mass, kg
m_s/m_o	Solidified mass fraction, ---
$\dot{Q}_{ch}$	Charging rate, kW
Q_{st}	Accumulative energy stored, kJ
$r_{avg_{h,v}}$	Average radius of solid–liquid interface in test capsule, m
r_h	Horizontal radius of solid–liquid interface in test capsule, m
r_{in}	Inside radius of test capsule, m
r_v	Vertical radius of solid–liquid interface in test capsule, m
h	Vertical distance, measured from the centre of the spherical capsule to the free surface of the encapsulated PCM, m
T_l	Liquid phase temperature of PCM, ^oC
T_o	Initial temperature of PCM (distilled water), ^oC
T_{pc}	Phase change temperature, ^oC
T_s	Solid phase temperature of PCM, ^oC
t	Time, min
Δt	time difference, s
V_s	Solidified volume, m^3
V_{PCM}	Spherical shell volume, m^3
$V_{capsule}$	Internal volume of the capsule m^3
$\dot{V}$	Actual volume flow rate, Lpm

Abbreviations

PCM:	Phase Change Material.
HTF:	Heat Transfer Fluid.
NFPCM:	Nano fluid Phase Change Material.
CTES:	Cool Thermal Energy Storage.
MWCNT:	Multi Wall Carbon Nanotubes.
DI:	De-ionized water.
LDPE:	Low Density Polyethylene.
$AL_2O_{3:}$	Aluminium Oxide.
LPM:	Litre Per Min.
LHTES	Latent heat thermal energy storage

Greek symbols

ρ_w	Water density, kg/m^3.
ρ_i	Ice density, kg/m^3.
ρ	Volume correction factor.

2. Experimental setup

A full vapour compression cycle as the main heart of the test rig was set up and indicated with the red colour in the schematic diagram shown in figure 1-a. The main purpose of this cycle is to cool down the heat transfer fluid (HTF) down to the desirable temperature (-6, -8, -10, and -12)˚C with a flow rate of 12 LPM. The other loop (Storage loop) indicated by cyan colour in figure 1-a

represents the cooling circuit for the encapsulated sphere. It consists of a pump forcing the HTF through the charging tank which contain the spherical capsule (test section). HTF used in experiments is composed (50-50) % wt. of (Ethylene glycol and water) and having a freezing point of -25 ̊C.

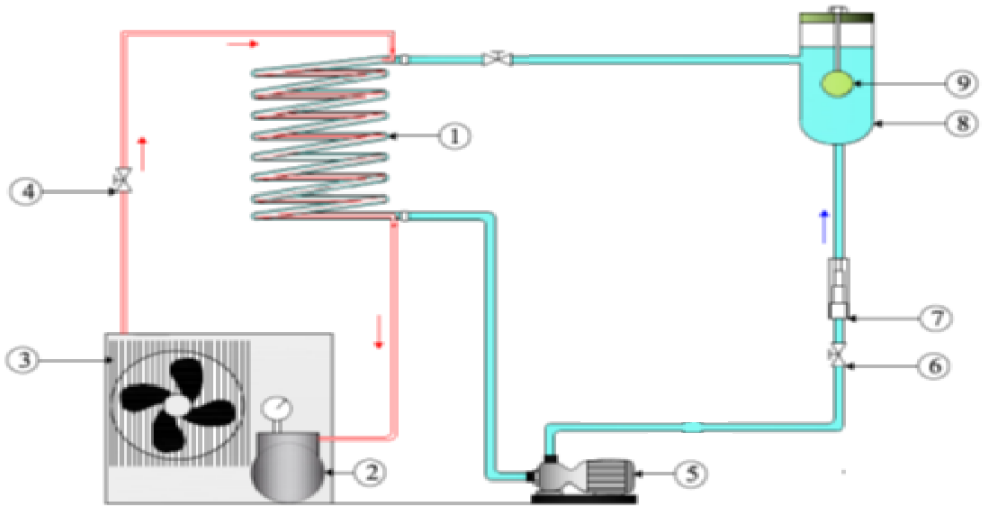

1- Evaporator 2- Compressor 3- Condenser 4- Expansion valve 5- pump
6- Gate valve 7-Rotameter 8- Discharging tank 9- Test section

Figure 1-a: Schematic diagram of the used test rig.

The cooling loop for the HTF consists of a simple vapour compression cycle which consists of compressor of 3 HP, forced air cooling condenser, thermal expansion valve and a tube in tube heat exchanger works as an evaporator of 1 ton refrigeration cooling capacity. The temperature was controlled using a digital thermostat to adjust and set the HTF temperature.

The storage loop consists of a cylindrical shape tank of 200 mm diameter and 900 mm height. The tank was insulated with glass wool insulation of 50 mm thickness. The HTF volume flow rate controlled and measured by manual gate valve, an aligned rota meter and HTF temperature was measured and controlled by digital temperature controller which having probe immersed in the HTF solution. 1 HP centrifugal pump forcing the HTF through the charging tank from HTF tube side in the evaporator section, Figure 1-b represents a photo for the assembled test rig.

Figure 1-b: Experimental test rig.

A copper spherical capsule of external diameter 84 mm and with 2 mm wall thickness was used as a PCM capsule (test section). The capsule was filled with 80% of its internal volume with De Ionized water (DI) as PCM to allow the warm development during the icing process [19] and to allow a space for water expansion volume expansion during the freezing process.

The internal surface roughness was made by the sand blasting technique with different grain sizes to achieve four different internal sphere surface roughness parameters (0, 3, 7 and 12) μm and the internal surface roughness was measured by surface profilometer (model: MITUTOYO SURF. TEST 301, as shown in figure 2) in Egypt Nuclear Energy Authority.

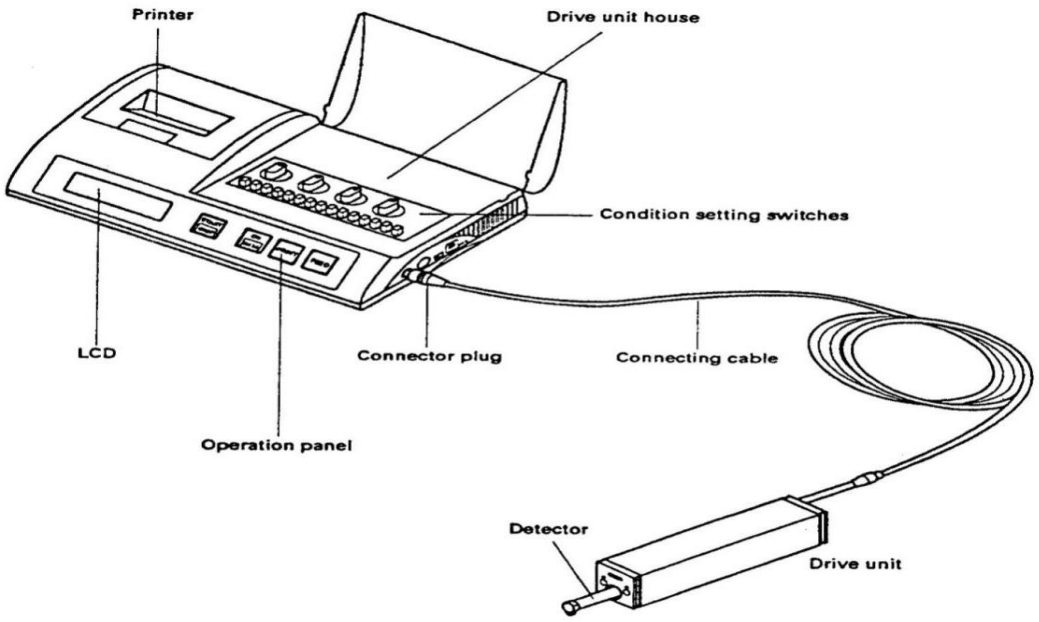

Figure 2: Surface profilometer

Nine calibrated T-type thermocouples were distributed over equal spacing positions along the horizontal and vertical tomahawks of the internal sphere as shown in figure 3. These thermocouples were connected into a data acquisition data acquisition unit to read the specimen temperatures and a core i7 PC was used to save the readings over time. The aim of this distribution is to indicate the temperature changes through the solidification process. Figure 4 represents a photo for the actual capsule after inserting thermocouples.

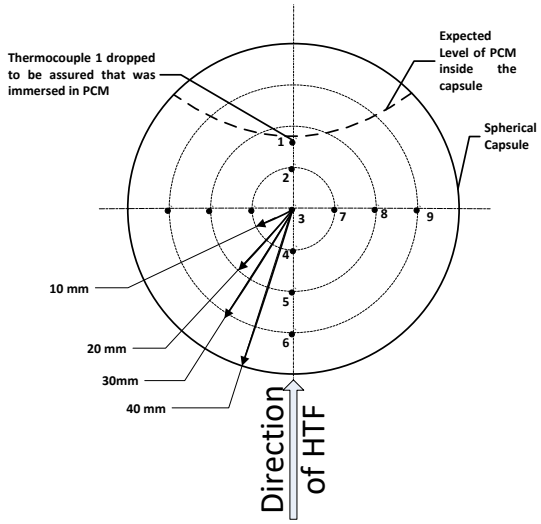

Figure 3: Distribution of thermocouples inside the PCM capsule.

Figure 4: Test section after applying thermocouples

Before starting experiments, PCM temperature was kept at 22˚C. The vapour compression cycle and the pump were turned on allowing the heat transfer fluid to be cooled in the evaporator section. Once achieving the required HTF temperature, the volume flow rate of the HTF was adjust and set at the desired value 12 LPM by manual valve. Afterwards, the PCM capsule was immersed and suspended at the local point of the tank.
The internal temperatures of the PCM were recorded at different positions until reaching the same temperature of the HTF at all measuring points. This demonstrates that the water was totally solidifies and the ice was being sub-cooled.
The thermocouples were set in the illustrated positions to specify the solidified volume of PCM with experiment time and get r_h and r_v then get $r_{avg..h,v}$ and finally get the solidified volume at any time through the experiment.

Measuring devices specifications used in this study are presented in table 1.

Table 1: measuring devices specifications

Thermocouples	Type	T-Type
	Range	-270 to 370 ℃
	Accuracy	±0.5 ℃
Data loggers	Type	NI 6210
	Sampling rate	250 kS/s
	Accuracy	±0.2%
Digital thermostat	Type	Eliwell 901
	Accuracy	±0.5%
Rota meter	Type	P520/530 Acrylic Rota meter
	Accuracy	±2%

3. Experimental errors and uncertainties

Using the accuracy values given in table 1, the uncertainty for the calculated quantities were calculated using the following formula that has been presented by Kline and McClintock, which is described in Holman [22].

$$e_r = \left[\left(\frac{\partial R}{\partial V_1} e_{v1}\right)^2 + \left(\frac{\partial R}{\partial V_2} e_{v2}\right)^2 + \cdots + \left(\frac{\partial R}{\partial V_n} e_{vn}\right)^2\right]^{0.5} \qquad \text{Eqn.1}$$

The uncertainty value was calculated to be 2.78% or less which is acceptable value for low hazard application (less than 5%).

3.1 Uncertainty in Solidified/Melted Mass Fraction

The solidified mass fraction is calculated from the following equation:

Solidified mass fraction= $\frac{m_s}{m_o} = \frac{\rho_i . V_s}{\rho_w . V_o}$

Assuming that the properties of PCM in both liquid and solid phases are constant:

$\therefore \frac{m_s}{m_o} = f(V_s, V_o)$

Therefore, the relative uncertainty in the solidified mass fraction is calculated as follows:

$$\frac{\omega_{(m_s/m_o)}}{\left(\frac{m_s}{m_o}\right)} = \sqrt{\left(\frac{\partial\left(\frac{m_s}{m_o}\right)/\partial V_s}{\left(\frac{m_s}{m_o}\right)}\omega_{V_s}\right)^2 + \left(\frac{\partial\left(\frac{m_s}{m_o}\right)/\partial V_o}{\left(\frac{m_s}{m_o}\right)}\omega_{V_o}\right)^2}$$

$$\frac{\omega_{(m_s/m_o)}}{\left(\frac{m_s}{m_o}\right)} = \sqrt{\left(\frac{\rho_i/\rho_w V_o}{\rho_i V_S/\rho_w V_o}\omega_{V_s}\right)^2 + \left(\frac{-\rho_i V_S/\rho_w V_o^2}{\rho_i V_S/\rho_w V_o}\omega_{V_o}\right)^2}$$

$$\frac{\omega_{(m_s/m_o)}}{\left(\frac{m_s}{m_o}\right)} = \sqrt{\left(\frac{\omega_{V_s}}{V_s}\right)^2 + \left(\frac{\omega_{V_o}}{V_o}\right)^2}$$

4-a. Data Reduction:

After reaching the set temperature for all the internal measuring points, the collected data including temperature versus time were used to calculate the solidified volume and mass, solidified mass fraction, accumulated energy stored and the charging rate as follow:

The solidified volume was calculated based on equation 2 below:

$$V_s = \rho\left(\frac{\rho_w}{\rho_i}\right)(2/3)\pi\left(r_{in}^3 - r_{avg_{h,v}}^3\right) + \pi h\left(r_{in}^2 - r_{avg_{h,v}}^2\right) \quad (m^3) \qquad \text{Eqn.2}$$

Where;

ρ_w *is the water density* kg/m^3

ρ_w *is the ice density* kg/m^3

r_{in} *is* Inside radius of test capsule, m

$r_{avg_{h,v}}$ *is* average radius of the solid − liquid interface inside the capsule

While the $r_{avg_{h,v}}$ is the average radius of the solid-liquid interface inside the capsule and was calculated by:

$$r_{avg_{h,v}} = \frac{r_h + r_v}{2} \quad (m) \qquad \text{Eqn.3}$$

Where;

r_h *is* Horizontal radius of solid– liquid interface in test capsule, m

r_v *is* Vertical radius of solid– liquid interface in test capsule, m

The solidified mass was calculated based on the density using equation 4.

$$m_s = \rho_i * V_s \quad (kg) \qquad \text{Eqn.4}$$

The solidified mass fraction was then calculated from:

solidified mass fraction = $m_s/(\rho_w * V_{PCM})$ ---- Eqn.5

Where;

V_{PCM} *is* Spherical shell volume, m^3 was taken as 80% of the capsule volume

The accumulated thermal energy stored within the test capsule was estimates as follow:

$$Q_{st} = \rho_w * V_{PCM} \left\{c_w(T_o - T_l) + \left(\frac{m_s}{m_o}\right) * L.H + \left(\frac{m_s}{m_o}\right) c_i\left(T_{pc} - T_s\right)\right\} \text{ (kJ)} \qquad \text{Eqn.6}$$

Where; T_o *is* Initial temperature of PCM (distilled water), ^{o} C
T_l is Liquid phase temperature of PCM, ^{o}C
$L.H$ *is* Latent heat of fusion of water, kJ/kg.
c_i & c_w *is* Specific heat of ice and water respectively, kJ/kg. K
T_{pc} *is* Phase change temperature, ^{o} C
T_s *is* Solid phase temperature of PCM, ^{o} C
$\left(\frac{m_s}{m_o}\right)$ *is the* solidified mass fraction $---$

The percentage of energy stored calculated by equation 7.

$$\%\, Q_{st} = [Q_{st}/Q_{st,max}]x100 \qquad \% \qquad \text{Eqn.7}$$

Where; $Q_{st,max}$ *is maximum energy stored*

The charging rate of thermal energy stored within the test capsule was finally calculated using equation 8.

$$\dot{Q}_{st} = \frac{\Delta Q_{st}}{\Delta t} \qquad \text{(kW)} \qquad \text{Eqn.8}$$

Where; Δt is the time interval, s

4-b. Sample of calculation

Figure 4-1. showing the plotting the temperature profiles for thermocouples inside the capsule.

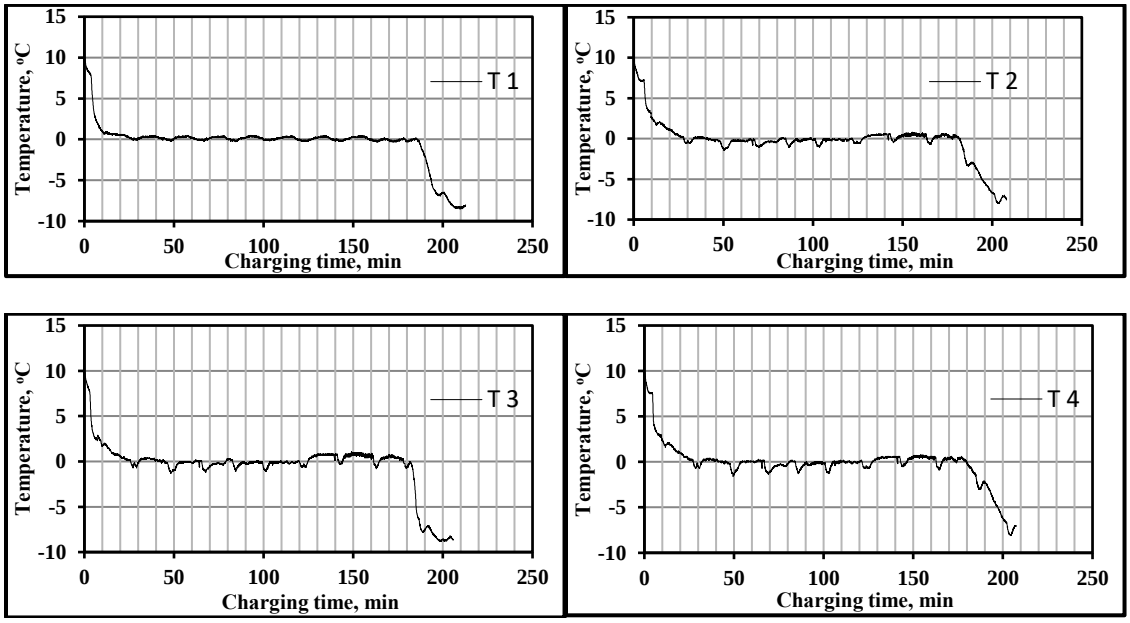

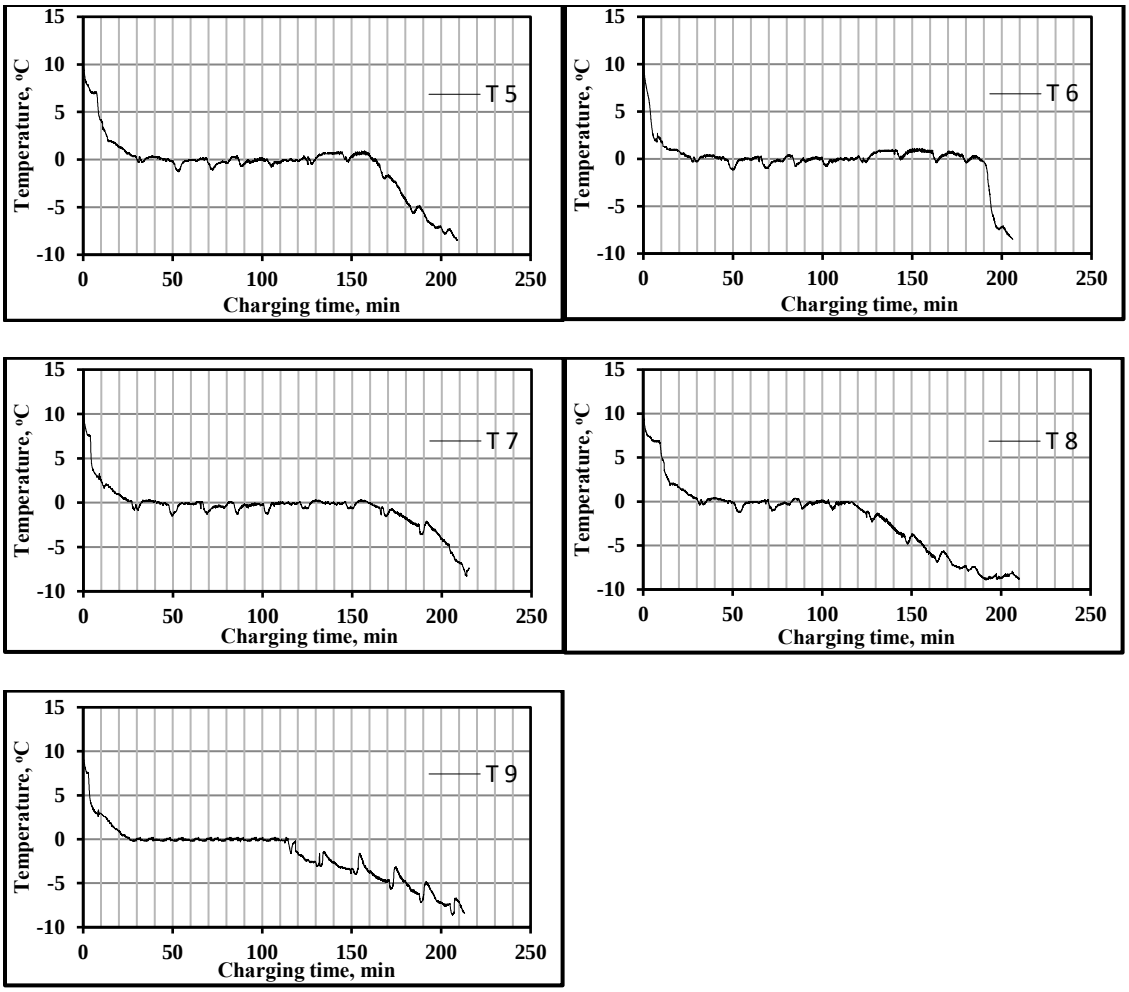

Figure 4.1: Temperature profiles for different thermocouples inside the capsule

Table 4-1. Determination the position of interface between solid and liquid using the temperatures profiles

T.C. No.	Time, min	rh (cm)	T.C. No.	Time, min	r_v (cm)
	0	4		0	4
6	37	3	9	34	3
5	79	2	8	75	2
4	115	1	7	111	1
3	155	0	1	155	0

Figure 4-2. and Figure 4-3. shown the relation between the position of solid-liquid interface and the time.

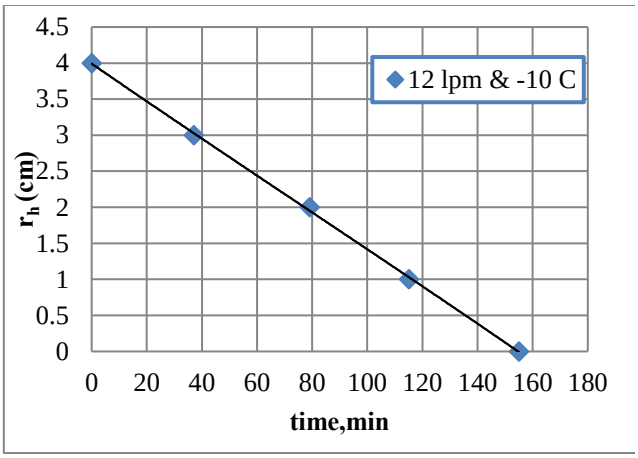

Figure 4.2: Variation of horizontal radius of solid–liquid interface with time

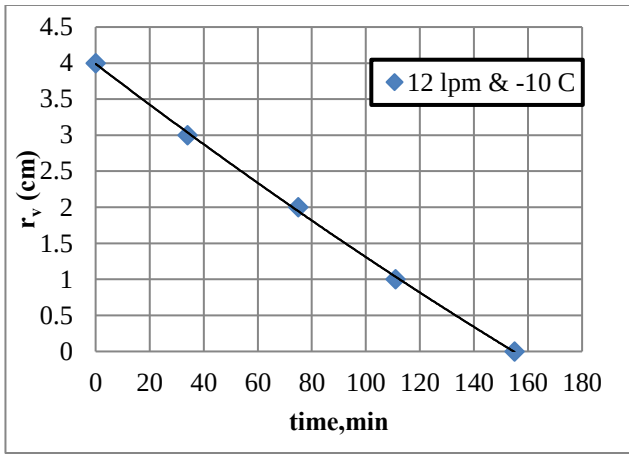

Figure 4.3: Variation of vertical radius of solid–liquid interface with time

Table 4-2. Deducing the position of interface at certain time intervals using the curve fitting equations.

Time, min	**rh (cm)**	***rv***
0	4	*4*
5	3.85	*3.85*
30	3.2	*3.15*
60	2.5	*2.4*
90	1.65	*1.5*
120	0.9	*0.85*
150	0.1	*0.1*
155	0	*0*

The properties of PCM (distilled water) in both liquid and solid phases, used in the present study, are listed in Table 4.3; It is assumed that the properties have constant values.

Table 4.3: properties of PCM (distilled water)

Property	**Water at 0 ºC**	**Ice at 0 ºC**
Density	ρ_w =1000 kg/m^3	ρ_i =920 kg/m^3
Specific Heat	C_w = 4.23 kJ/kg.K	C_i =2.04 kJ/kg.K
Latent heat	L.H.=333.7 kJ/kg	L.H.=333.7 kJ/kg
Thermal conductivity		k_i =1.88 W/m.K
Thermal diffusivity		α_i =1.0017 x 10-6 m^2/s

4-c. Calculations sample and steps

Table 4.4. calculations of Solidified mass fraction

Time, min	r_{in}	r_h	r_v	$r_{avg(h,v)}$	h	$V_s = (\rho_w/\rho_i)((2/3) * \pi * (r_{in}^3 - r^3_{avg,(h,v)}) + \pi * h * (r_{in}^2 - r^2_{avg,(h,v)}))$ (cm^3)	$ms=\rho i*Vs$	$m_o=\rho w*Vcap$	m_s/m_o
0	4	4	4	4	1.6	0	0	214466	0
5	4	3.85	3.85	3.85	1.6	22.36256974	20573.56	214466	0.0959293
30	4	3.2	3.15	3.175	1.6	105.7081264	97251.48	214466	0.4534587
60	4	2.5	2.4	2.45	1.6	167.4111463	154018.3	214466	0.7181477
90	4	1.65	1.5	1.575	1.6	210.9841832	194105.4	214466	0.905064
120	4	0.9	0.85	0.875	1.6	227.4601075	209263.3	214466	0.9757411
150	4	0.1	0.1	0.1	1.6	232.9428898	214307.5	214466	0.9992608
155	4	0	0	0	1.6	232.9970294	214357.3	214466	0.999493
191	4	0	0	0	1.6	232.9970294	214357.3	214466	0.999493

Table 4.5. calculations of Percentage of energy stored

Time, min	τ	ms/mo	(To-Tl)	(Tpc-Ts)	$Q_{st}=\rho_w.V_o[C_w.(T_o-T_l)+(m_s/m_o)(L.H.)+(m_s/m_o)C_i(T_{pc}-T_s)]$ (kJ)	$\% Q_{st} = (Q_{st}/Q_{st,max})x100$
0	0	0	0	0	0	0
5	0.1878	0.095929	5	0	11.37658096	11.8935
30	1.1269	0.453459	22	0.5	52.39612388	54.7768
60	2.2538	0.718148	22	2	71.82608565	75.0896
90	3.3807	0.905064	22	3.8	86.0485229	89.9583
120	4.5077	0.975741	22	4.6	91.55373092	95.7136
150	5.6346	0.999261	22	5.3	93.58590728	97.8381
155	5.8224	0.999493	22	5.7	93.77756505	98.0385
191	7.1747	0.999493	22	10	95.65382132	100

Table 4.6. calculation of the Charging rate

Time, min	τ	Q_{st} (kJ)	$\dot{Q}_{st} = \Delta Q_{st} / \Delta t$
0	0	0	0
5	0.1878	11.37658	0.0379219
30	1.1269	52.39612	0.0273464
60	2.2538	71.82609	0.0107944
90	3.3807	86.04852	0.0079014
120	4.5077	91.55373	0.0030584
150	5.6346	93.58591	0.001129
155	5.8224	93.77757	0.0006389
191	7.1747	95.65382	0.0008686

5. Results and Discussion

Figures 5.a, 5.b, 5.c and 5.d represents the solidified mass fraction versus time at different HTF temperatures of (-6, -8, -10 and -12)˚C respectively for different internal surface roughness values.

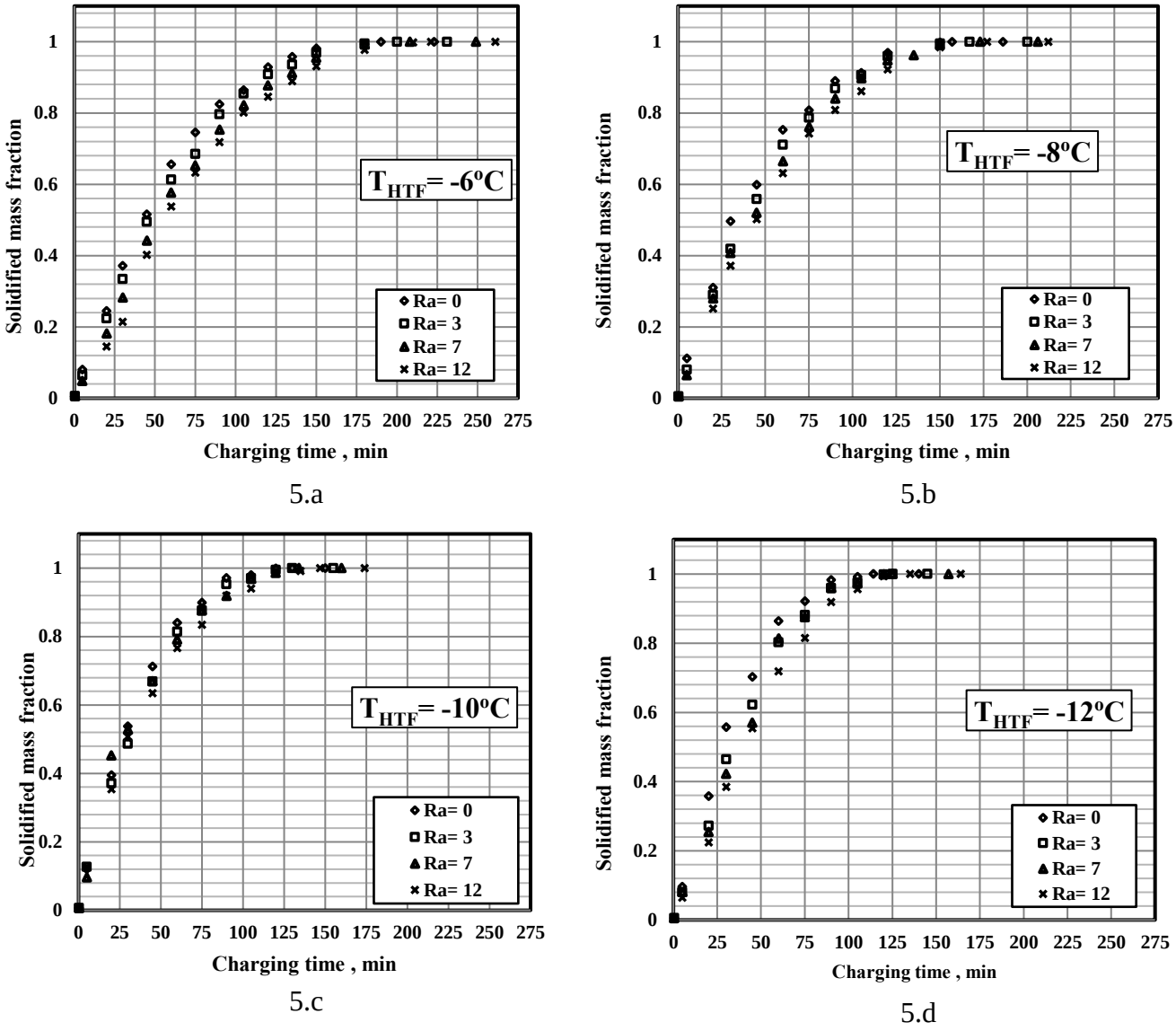

5.a 5.b

5.c 5.d

Figure 5: Solidification mass fraction versus charging time at different heat transfer fluid temperature fo different surface roughness.

By analysing figure (5), it can be noted that at all heat transfer fluid temperatures the surface roughness has a negative effect on the charging time and the solidified mass faction. By increasing the surface roughness, the charging time increases and reaching the maximum value at the highest tested surface fraction and consequently at the same charging time, the smoother surface had a higher solidification mass fraction. This adverse effect on the freezing performance occurred due to the roughness negative effect on nucleation formation. Also, by increasing the surface roughness, the thermal contact resistance between the adjacent formed ice layer and the internal capsule surface increases hence increasing the overall thermal resistance and decreasing the heat transfer from the HTF and the encapsulated material.

It is depicted from the figure that by decreasing the HTF inlet temperature, the complete time for solidification process decreases. For HTF inlet temperatures of -6 ̊C, -8 ̊C, -10 ̊C, and -12 ̊C, the total time required for complete solidification was recorder to be of 160, 150, 125 and 100 minutes respectively. This happened due to the higher thermal potential of the heat transfer process using lower HTF temperatures.

As a reflection, the effect of surface roughness on temporal variation of energy stored percentage for inlet HTF temperature of temperature -6 ̊C, -8 ̊C, -10 ̊C, and -12 ̊C has the same variation trend with time as shown in figures 6a, 6.b, 6.c and 6.d, respectively. That's because the major part of heat stored is latent heat of freezing.

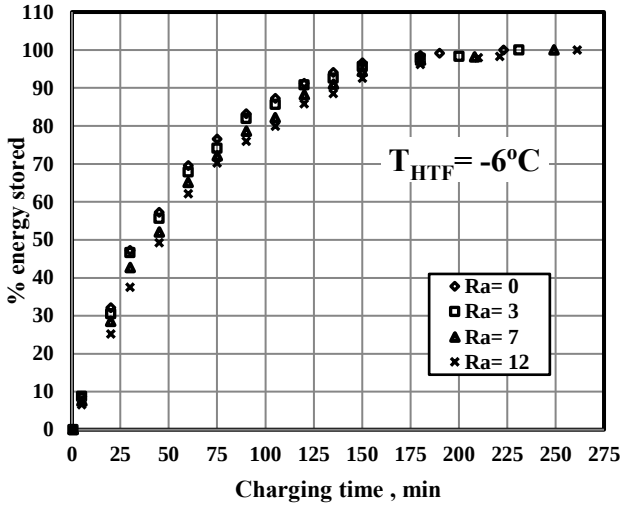

6.a

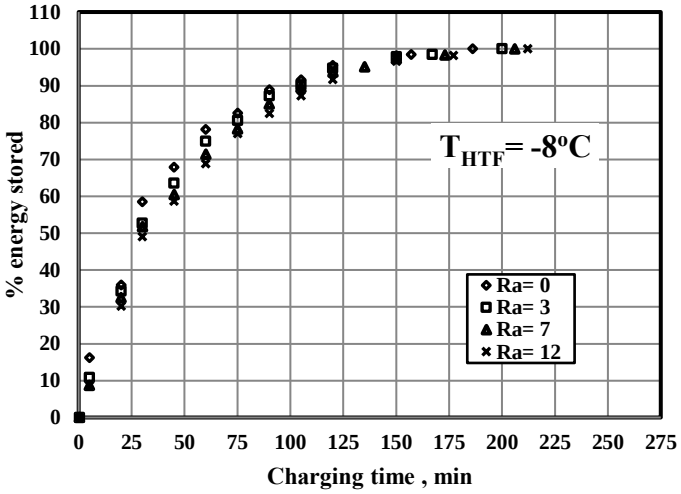

6.b

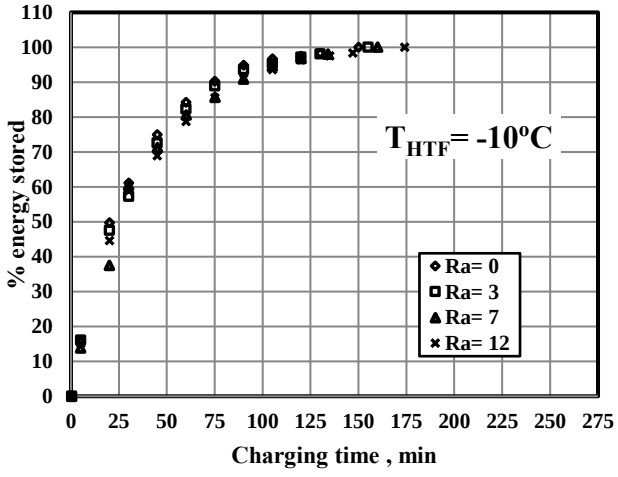

6.c

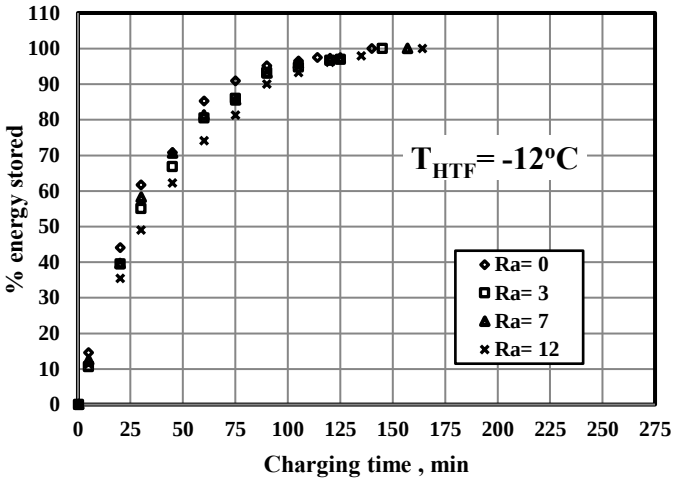

6.d

Figure 6: Effect of surface roughness on energy stored rate at various heat transfer fluid temperature

Figure 7.a, 7.b, 7.c and 7.d represents the charging rate versus charging time at the tested HTF inlet temperatures of (-6, -8, -10 and -12)˚ C respectively for different internal surface roughness values.

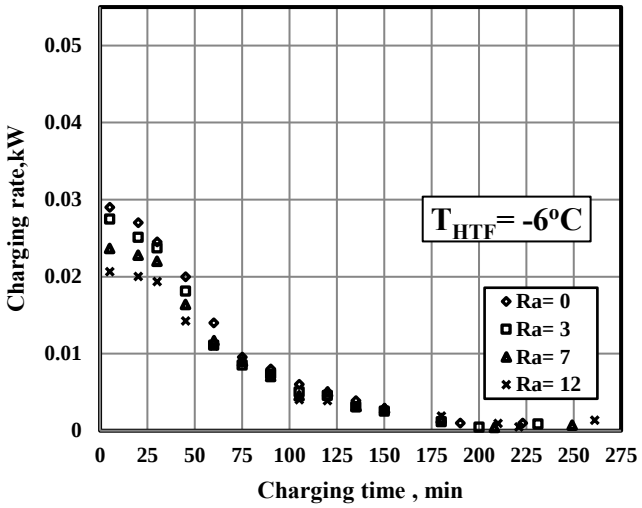

7.a

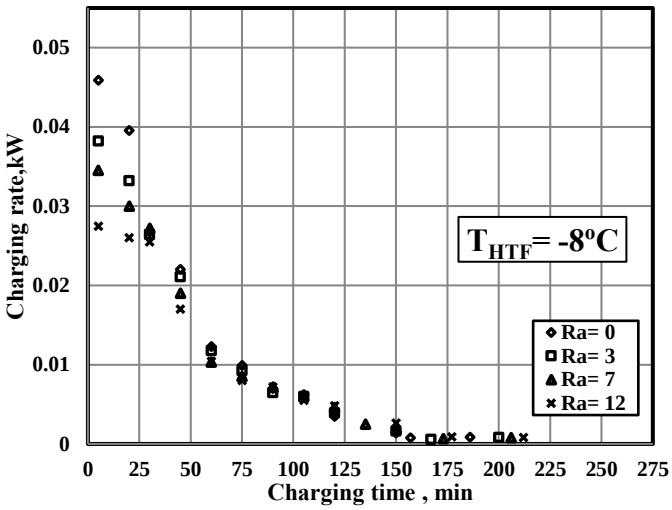

7.b

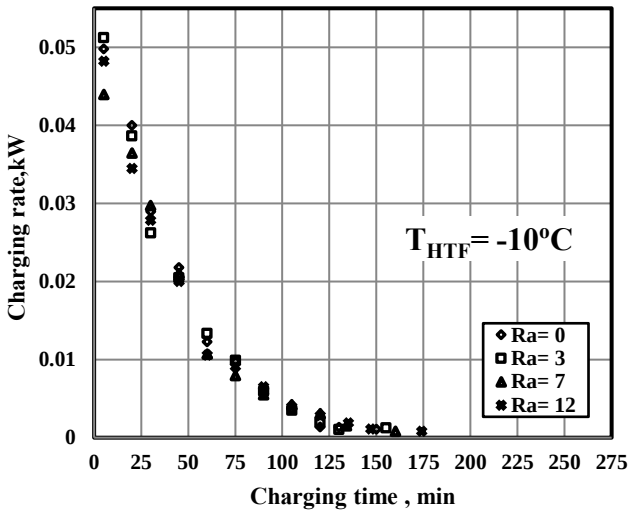

7.c

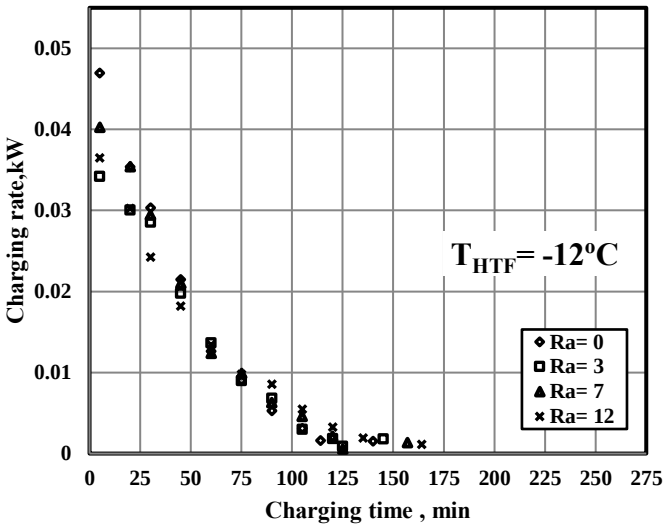

7.d

Figure 7: Effect of surface roughness on charging rate at various heat transfer fluid temperature.

From above figures, it can be noted that at different inlet temperature for heat transfer fluid, the charging time decreases by decreasing HTF inlet temperature. It was also noticed that the surface roughness has a significant effect at the early stages of the freezing process t≤50 minutes for HTF temperatures of -6˚C and -8˚C and t≤25 minutes for HTF temperatures of -10˚C and -12˚C. Also, from the figure it is clear that the complete charging time for inlet HTF temperature decreases by 75 minutes while using HTF inlet temperature of -12˚C compared with using HTF temperature of -6˚C. This is due to the higher temperature difference between the HTF temperature and the encapsulated water which led to higher heat transfer potential.

Finally, and for better comparison, the complete charging time variation was plotted versus surface roughness as shown in figure 8. This figure shows and summarises the direct proportional relation between the complete charging time and the surface roughness.

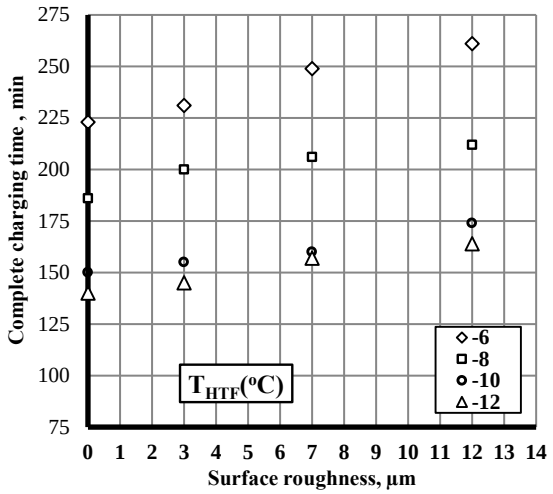

Figure 8: Complete charging time versus surface roughness.

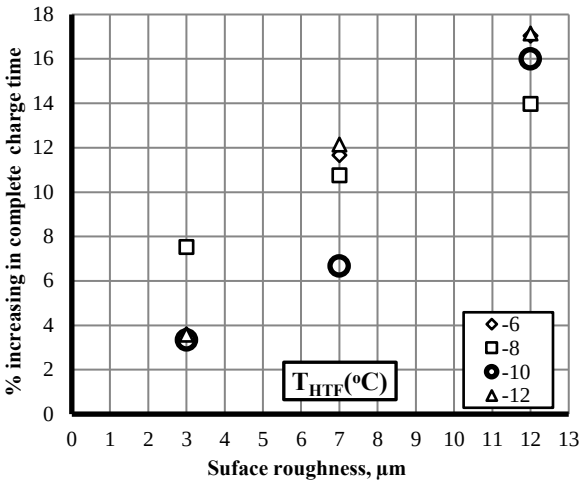

Figure 9: Percentage increase in complete charging time versus surface roughness.

Figure (8) shows that the complete charging time variation with surface roughness. The complete charging time increase with the increase in surface roughness for all temperature. This due to the increase time that used in nucleation process as previously mentioned. The more the temperature decrease the variation rate increases with the increase in surface roughness see figure (9). For constant temperature of heat transfer fluid, the trend line slope angle decreases with the decrease of temperature of heat transfer fluid. i.e the slop for heat transfer fluid temperature at -6℃ is greater than that of HTF inlet temperature at -12 °C. see figure (9). From figure (8), (9) it could be summarise that the direct proportional relation between the complete charging time and the surface roughness

6. Conclusion:

The effect of encapsulated material internal surface roughness on the energy stored, solidification mass fraction and total charging time is well discuss. Four different surface roughness of (0,3,7 and 12) µm were tested at different heat transfer fluid temperatures ranging between (-6 to -12) ° C. Results showed that the more internal surface roughness, the more the charging time due to difficulties of ice nuclei formations on rough surfaces and the increase of surface contact resistance. The trend line slope for complete charging time variation versus surface roughness showed the linear direct relation between the charging time and surface roughness. Finally it is recommended to use a purely smooth surface for encapsulated cooling application for more stable ice nucleation and less charging time.

7. REFRENCES:

[1] Oró, E., de Gracia, A., Castell, A., Farid, M. M. and Cabeza, L. F. (2012) "Review on Phase Change Materials (pcms) for Cold Thermal Energy Storage Applications," **Applied Energy**, 99, pp. 513–533. doi: 10.1016/j.apenergy.2012.03.058.

[2] Li, G., Hwang, Y., Radermacher, R. and Chun, H.-H. (2013) "Review of Cold Storage Materials for Subzero Applications," **Energy**, 51, pp. 1–17. doi: 10.1016/j.energy.2012.12.002.

[3] Raja S, Prakash S, Gokulnath R, Krishnamoorthy A and Lillymercy J (2018) "Pcm Based Thermal Energy Storage System Integrated with Solar Parabolic Trough Collector," Journal of Engineering Science and Technology, 13(Special Issue On The Ninth Eureca 2017), pp. 40–51.

[4] Song, M., Niu, F., Mao, N., Hu, Y. and Deng, S. (2018) "Review on Building Energy Performance Improvement Using Phase Change Materials," Energy and buildings, 158, pp. 776–793.

[5] Alizadeh, M. and Sadrameli, S. M. (2016) "Development of Free Cooling Based Ventilation Technology for Buildings: Thermal Energy Storage (TES) Unit, Performance Enhancement Techniques and Design Considerations - a Review," **Renewable and Sustainable Energy Reviews**, 58, pp. 619–645. doi: 10.1016/j.rser.2015.12.168.

[6] Panchabikesan, K., Vellaisamy, K. and Ramalingam, V. (2017) "Passive Cooling Potential in Buildings Under Various Climatic Conditions in India," **Renewable and Sustainable Energy Reviews,** 78, pp. 1236–1252. doi: 10.1016/j.rser.2017.05.030.

[7] Tay, N. H. S., Liu, M., Belusko, M. and Bruno, F. (2017) "Review on Transportable Phase Change Material in Thermal Energy Storage Systems," **Renewable and Sustainable Energy Reviews**, 75, pp. 264–277. doi: 10.1016/j.rser.2016.10.069.

[8] Said, M. A. and Hassan, H. (2018) "Parametric Study on the Effect of Using Cold Thermal Storage Energy of Phase Change Material on the Performance of Air-Conditioning Unit," **Applied Energy**, 230, pp. 1380–1402. doi: 10.1016/j.apenergy.2018.09.048.

[9] Yan, C., Shi, W., Li, X. and Zhao, Y. (2016) "Optimal Design and Application of a Compound Cold Storage System Combining Seasonal Ice Storage and Chilled Water Storage," **Applied Energy**, 171(1 June 2016), pp. 1–11.

[10] Cheng, X. and Zhai, X. (2018) "Thermal Performance Analysis and Optimization of a Cascaded Packed Bed Cool Thermal Energy Storage Unit Using Multiple Phase Change Materials," **Applied Energy**, 215, pp. 566–576. doi: 10.1016/j.apenergy.2018.02.053.

[11] Yu, Q., Tchuenbou-Magaia, F., Al-Duri, B., Zhang, Z., Ding, Y. and Li, Y. (2018) "Thermo-Mechanical Analysis of Microcapsules Containing Phase Change Materials for Cold Storage," **Applied Energy**, 211, pp. 1190–1202. doi: 10.1016/j.apenergy.2017.12.021.

[12] Panchabikesan, K., Vincent, A. A. R., Ding, Y. and Ramalingam, V. (2018) "Enhancement in Free Cooling Potential through Pcm Based Storage System Integrated with Direct Evaporative Cooling (dec) Unit," **Energy**, 144, pp. 443–455. doi:0.1016/j.energy.2017.11.117.

[13] Pomianowski, M., Heiselberg, P. and Zhang, Y. (2013) "Review of Thermal Energy Storage Technologies Based on Pcm Application in Buildings," **Energy & Buildings**, 67, pp. 56–69. doi: 10.1016/j.enbuild.2013.08.006.

[14] Safari, A., Saidur, R., Sulaiman, F. A., Xu, Y. and Dong, J. (2017) "A Review on Supercooling of Phase Change Materials in Thermal Energy Storage Systems," **Renewable and Sustainable Energy Reviews**, 70, pp. 905–919. doi: 10.1016/j.rser.2016.11.272.

[15] Liu, S., Li, H., Song, M., Dai, B. and Sun, Z. (2018) "Impacts on the Solidification of Water on Plate Surface for Cold Energy Storage Using Ice Slurry," **Applied Energy**, 227, pp. 284–293. doi: 10.1016/j.apenergy.2017.08.012.

[16] Akio, Yoshio, S., Seiji, U., Kazuyuki, O. and Atsushi, M. (1990) "Fundamental Research on the Supercooling Phenomenon on Heat Transfer Surfaces—investigation of an Effect of Characteristics of Surface and Cooling Rate on a Freezing Temperature of Supercooled Water," **International Journal of Heat and Mass Transfer**, 33(8), pp. 1697–1709. doi: 10.1016/0017-9310(90)90025-P.

[17] Faucheux, M., Muller, G., Havet, M. and LeBail, A. (2006) "Influence of Surface Roughness on the Supercooling Degree: Case of Selected Water/ethanol Solutions Frozen on Aluminium Surfaces," **International Journal of Refrigeration**, 29(7), pp. 1218–1224. doi: 10.1016/j.ijrefrig.2006.01.002.

[18] Wang, X. J., Li, X. F., Xu, Y. H. and Zhu, D. S. (2014) "Thermal Energy Storage Characteristics of Cu-H2o Nanofluids," **Energy**, 78, pp. 212–217. doi: 10.1016/j.energy.2014.10.005.

[19] Liu, Y., Li, X., Hu, P. and Hu, G. (2015) "Study on the Supercooling Degree and Nucleation Behavior of Water-Based Graphene Oxide Nanofluids Pcm," **International Journal of Refrigeration**, 50, pp. 80–86. doi: 10.1016/j.ijrefrig.2014.10.019.

[20] P. Chandrasekaran a, M. Cheralathan a, R. Velraj (2015) "Influence of the size of spherical capsule on solidification characteristics of DI (deionized water) water for a cool thermal energy storage system - An experimental study ", **Energy**, 90 807-813.

[21] P. Chandrasekaran a, M. Cheralathan a, R. Velraj "Effect of fill volume on solidification characteristics of DI (deionized) water in a spherical capsule - An experimental study", **Energy** 90 (2015) 508-515.

[22] J. P. Holman, "Experimental Method for Engineers", 4th edition, New York: McGraw-Hill, 1984.